

Estimation of Time to Contact from Blurred Images

Yukitada Takanashi, Kazuyuki Ito

Dept. of Electrical and Electronics Engineering
HOSEI University

Tokyo, Japan

e-mail: 10x2061@stu.hosei.ac.jp, ito@hosei.ac.jp

Abstract— Recently, intelligent safety systems, such as autonomous collision avoidance for automobiles have attracted considerable attention. In this paper, we propose an algorithm that can estimate time to contact by using blurred images that are captured by a monocular camera rather than distance information. We conducted experiments in order to confirm the validity of the algorithm.

Keywords— ecological psychology; τ -margin; monocular camera; crush avoidance; blurred image; time to contact

I. INTRODUCTION

Recently, intelligent safety systems, such as autonomous collision avoidance for automobiles have attracted considerable attention. Automobiles are typically equipped with distance sensors or stereo cameras to detect obstacles in their path [1][2].

In conventional works, there are three major methods for measuring distance between the automobile and the obstacle [3]. Table I shows the features of the three major methods.

TABLE I. FEATURES OF THE MAIN METHODS TO MEASURE AUTOMOBILE-OBSTACLE DISTANCE

	Bad weather environment	Dark conditions	Cost
Stereo camera	Not-applicable	Not-applicable	Middle
Laser radar	Not-applicable	Applicable	Low
Millimeter-wave radar	Applicable	Applicable	High

In general, in order to measure distances in dark conditions, the cost to realize the system becomes high because a combination of the multiple methods is required in this case.

On the other hand, in the context of ecological psychology [4][5], it has been demonstrated that time to contact can also be estimated by simply using monocular visual information rather than distance information. In ecological psychology, time to contact is called tau-margin, and it can be calculated based on the apparent size of an approaching object and its temporal change [6].

In our previous studies, we proposed methods to estimate tau-margin using the images of a monocular camera [7]. However, in dark conditions, such as those at night, it was very difficult to estimate tau-margin because of blurred images.

To address this issue, in this paper, we propose an algorithm that can estimate the tau-margin at night despite blurred images acquired from monocular camera.

We conducted experiments in order to confirm the validity of the algorithm.

The rest of the paper is organized as follows. Section II introduces the tau-margin. Section III describes our proposed algorithm tau-margin using blurred images. Section IV verifies the proposed algorithm. Section V concludes this paper.

II. TAU-MARGIN

Figure 1 shows an object approaching a camera.

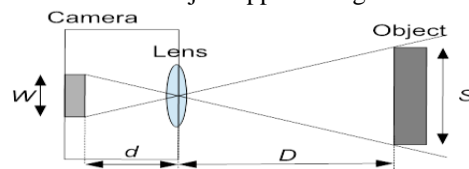


Figure 1. Appearance of the object.

The apparent size W can be expressed by (1). The temporal change \dot{W} is given by (2), where \dot{D} is the approaching speed.

Equation (3) is obtained from (1) and (2). Equation (3) implies that the time to contact $-D/\dot{D}$ is obtained from W/\dot{W} . In ecological psychology, W/\dot{W} is called tau-margin (τ).

$$W = \frac{d}{D} S \tag{1}$$

$$\dot{W} = -\frac{dS}{D^2} \dot{D} \tag{2}$$

$$-\frac{D}{\dot{D}} = \frac{W}{\dot{W}} (= \tau) \tag{3}$$

In our previous study [7], we estimated tau-margin based on the movement of each pixel. Figure 2 shows the movement of pixels and Figure 3 shows the coordinate system.

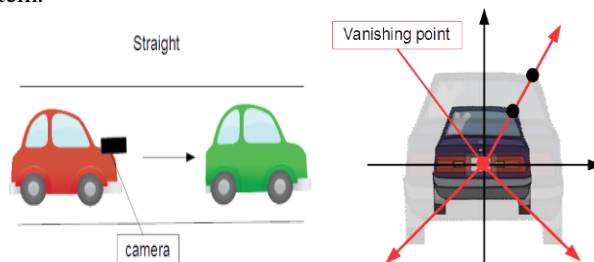


Figure 2. Movement of pixels.

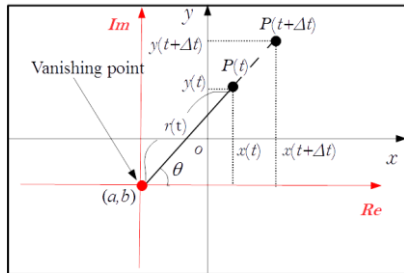


Figure 3. Coordinate system.

The center of the expanding image is called the vanishing point. In Figure 3, the origin of the polar coordinate system is the vanishing point. In the polar coordinate system, the expansion of an image is expressed by (4) and (7). The position of the vanishing point moves when the car turns. The movement of the vanishing point is expressed in the X-Y coordinate system in Figure 3. Thus, the movement of each pixel is given by (5) and (6), and (8) and (9), where Δt is the time interval.

$$P(t + \Delta t) = P(t) \left\{ 1 + \frac{\Delta t}{\tau(t)} \right\} \quad (4)$$

$$x(t + \Delta t) = \{x(t) - a\} \left\{ 1 + \frac{\Delta t}{\tau(t)} \right\} + a \quad (5)$$

$$y(t + \Delta t) = \{y(t) - b\} \left\{ 1 + \frac{\Delta t}{\tau(t)} \right\} + b \quad (6)$$

$$P(t - \Delta t) = P(t) \left\{ 1 + \frac{\Delta t}{\tau(t - \Delta t)} \right\}^{-1} \quad (7)$$

$$x(t - \Delta t) = \{x(t) - a\} \left\{ 1 + \frac{\Delta t}{\tau(t - \Delta t)} \right\}^{-1} + a \quad (8)$$

$$y(t - \Delta t) = \{y(t) - b\} \left\{ 1 + \frac{\Delta t}{\tau(t - \Delta t)} \right\}^{-1} + b \quad (9)$$

III. PROPOSED ALGORITHM

Figure 4 shows the setting of camera, and Figures 5-7 show the algorithm.

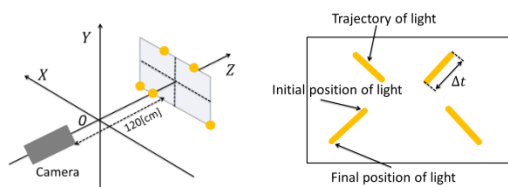


Figure 4. Setting of camera and its blurred image.

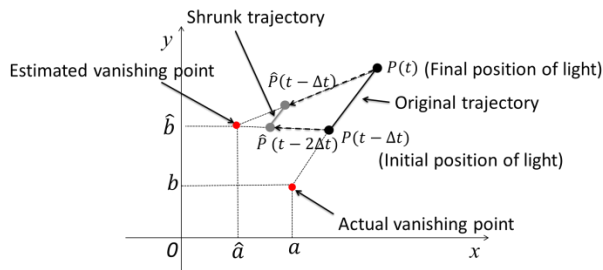


Figure 5. Estimated vanishing point.

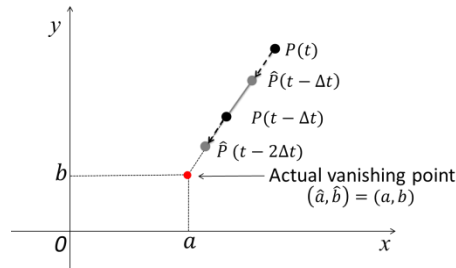


Figure 6. Reduce a locus of light.

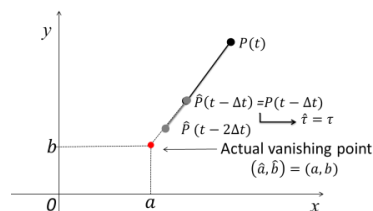


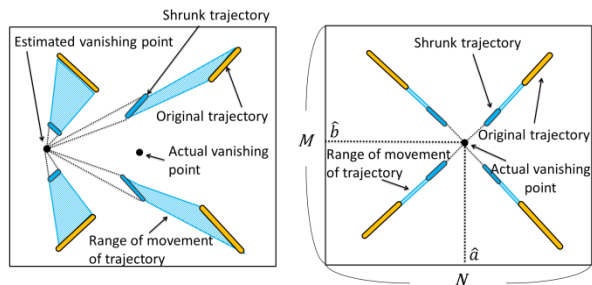
Figure 7. Acquisition of tau-margin.

In this study, we propose an algorithm that can estimate tau-margin using blurred images. Figure 4 shows an example of a blurred image captured in dark conditions. We assume that static point light sources are on the same plane perpendicular to the direction of camera's movement, and the trajectory of the point light source on the captured image is a straight line, as shown in Figure 4. We process the entire image without having to distinguish a point light sources. These trajectories include information on the movement of the moving camera. The inside edge of the trajectory is the initial position of the light and the other side is its final position.

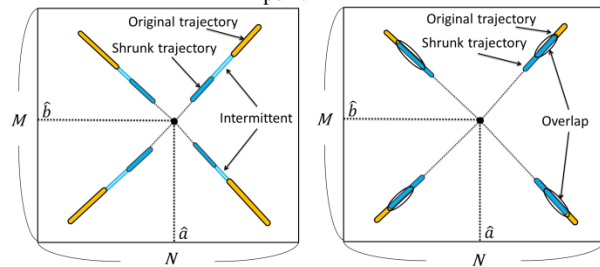
We estimate the vanishing point (a, b) using (8) and (9). First, we shrink the trajectory by substituting \hat{a} , \hat{b} , and $\hat{\tau}$ in (8) and (9), where \hat{a} , \hat{b} , and $\hat{\tau}$ are estimated values. Through trajectory shrinking, the trajectory moves to the estimated vanishing point (\hat{a}, \hat{b}) , as shown in Figures 5-7. As shown in Figure 5, when there is an erroneous position between the actual vanishing point and the estimated vanishing point, the shrunk trajectory does not lie on the original trajectory.

On the other hand, as shown in Figure 6, the estimated vanishing point and the actual vanishing point are the same. The shrunk trajectory moves to the original trajectory towards the actual vanishing point. By conforming the shrunk trajectory to the original trajectory, we can obtain the estimated values of \hat{a} , \hat{b} , and $\hat{\tau}$.

To estimate \hat{a} , \hat{b} , and $\hat{\tau}$, we employ the method of least squares. Figure 8 shows changes in the trajectory due to the position of the vanishing point.



(a) Vanishing point has error (b) Vanishing point has no error
Figure 8. Changes in the trajectory due to the position of the vanishing point



(a) Tau is too small (b) Tau is too large
Figure 9. Changes in the trajectory due to the value of tau

When there is an erroneous position between the actual vanishing point and the estimated position of the vanishing point, the trajectory shrinks, as shown in Figure 8 (a). On the other hand, when there is no error, the trajectory shrinks, as shown in Figure 8 (b).

By minimizing the area of the rectangle composed of the original trajectory and the shrunk trajectory, we obtain estimated position of the vanishing point (\hat{a}, \hat{b}) .

In the same way, as shown Figure 9, by minimizing the area of the overlaps and the intermittent between the original trajectory and the shrunk trajectory, we obtain the estimated time to contact $\hat{\tau}$. Figure 10 the flowchart of the theory and Table II defines the parameters used in the flowchart. In Figure 10, we employ the coordinate system in Figure 11.

TABLE II. PARAMETERS

$B(i, j)$	Binary image
$S(i, j)$	Shrink image
$S_a(i, j)$	Accumulation of shrink image
(i_b, j_a)	Position of vanishing point
M	Height of image
N	Width of image
R	Shrink rate
R_{max}	Upper limit of shrink rate
ΔR	Step size of R_{max}
Δt	Shutter speed
est_R	estimate value of R
est_i_b	estimate value of i_b
est_j_a	estimate value of j_a
est_tau	estimate value of time to contact τ
min_S_a	minimum value of sum of pixels of $S_a(i, j)$
min_dis	minimum value of sum of pixels of the overlaps and the intermittent between $B(i, j)$ and $S(i, j)$

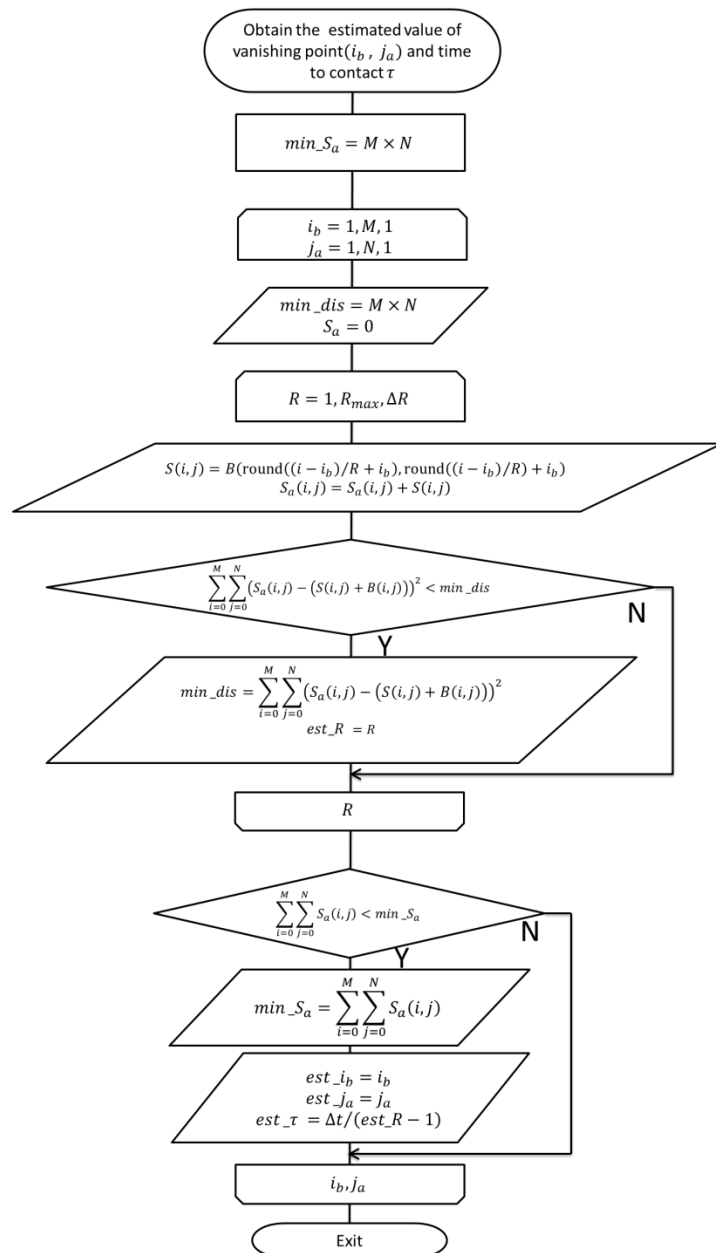
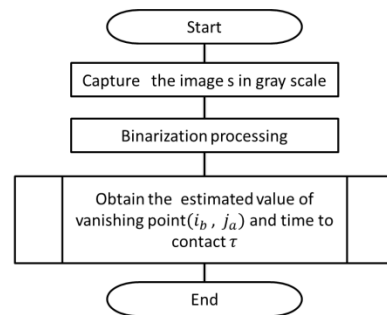


Figure 10. Flowchart of the theory

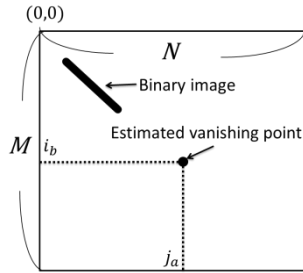


Figure 11. Coordinate system for captured image

IV. EXPERIMENT

We conducted an experiment to verify the basic capability of the proposed method. Table III shows the setting of the experiment. Processing was conducted offline. Processing time per image was approximately 90 seconds.

TABLE III. SPECS OF THE PC AND EXPERIMENT SETTING

OS	Windows 7 Enterprise
CPU	Intel(R) Core(TM) i3 1.33GHz
Memory	4GB
Application for calculation	MATLAB R2013a
Image size	150×300 [pixel]
Shutter speed of the camera	0.5 [sec]

The camera moved to the point light source by a constant speed, as shown in Figure 4. Figure 12 depicts the captured images. Figure 13 shows the estimated time to contact (\hat{t}). From Figure 13, we can confirm that the time to contact is successfully estimated.

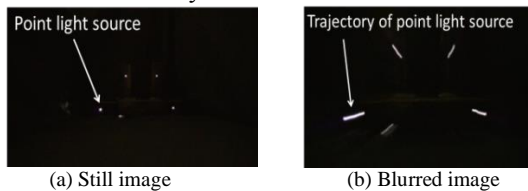


Figure 12. Five point light sources.

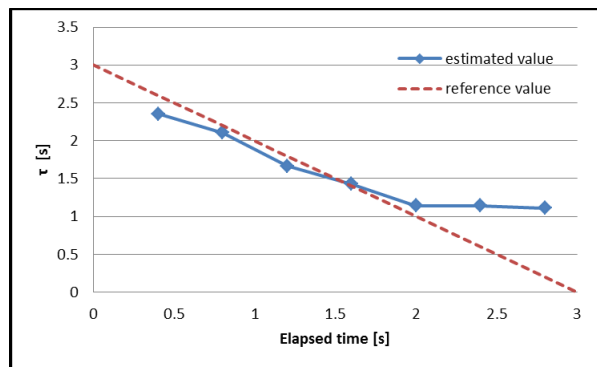


Figure 13. Experiment result.

V. CONCLUSION AND FUTURE WORK

In this paper, we focused on the framework of ecological psychology and we proposed a simple algorithm to estimate the time to contact using blurred images. In this algorithm, expansion of obstacles on captured images is estimated from the trajectories of point light sources on the blurred images, and the time to contact to the obstacles is obtained. Thus, the proposed algorithm is applicable to dark conditions.

To demonstrate the effectiveness of the proposed algorithm, an experiment in a simple dark condition was conducted and we confirmed that time to contact could be estimated.

In the future, we plan to apply the proposed approach to various types of real environment and verify its usability in that environment.

ACKNOWLEDGMENT

This research was partially supported by the Japan Society for the Promotion of Science through a Grant-in-Aid for Scientific Research (C), No. 24500181.

REFERENCES

- [1] I. Joung and I. Ahn, "Two-dimensional depth data measurement using an active omni-directional range sensor," IEICE Trans. Fund. Electron., Commun. Comp. Sci., vol. E84-A, no. 5, 2001, pp. 1288–1292.
- [2] B. D. Lucas and T. Kanade, "An Iterative Image Registration Technique with an Application to Stereo Vision", Proc 7th Intl Joint Conf on Artificial Intelligence, 1981, pp. 674-679.
- [3] Nikkei Electronics:NE Handbook series Sensor Networks: Nikkei Business Publications, Inc., June, 2014, pp. 16-19.
- [4] J. J. Gibson, "Reasons for Realism: Essays in Feminist Theory," Lawrence Erlbaum Associates, 1982.
- [5] J. J. Gibson, "The Ecological Approach to Visual Perception," Lawrence Erlbaum Associates, 1986.
- [6] D. N. Lee, "The optic flow field: The foundation of vision," Phil. Trans. Royal Soc. London B, vol. 290, no. 1038, 1980, pp. 169–179.
- [7] Y. Kawai and K. Ito, "Estimation Method for Time to Contact from Visual Information - A Simple Approach That Requires No Recognition of Objects -"International Conference, IEEE 2014, Bali, Indonesia, 5-10th December, Robotics and Biomimetics, 2014, pp. 469-474.